Rotationally invariant formulation of spin-lattice coupling in multiscale modeling

Markus Weißenhofer [1,*] Hannah Lange [2] Akashdeep Kamra [3] Sergiy Mankovsky [2]
Svitlana Polesya [2] Hubert Ebert [2] and Ulrich Nowak [1]

[1]*Department of Physics, University of Konstanz, DE-78457 Konstanz, Germany*
[2]*Department of Chemistry/Phys. Chemistry, LMU Munich, Butenandtstrasse 11, DE-81377 Munich, Germany*
[3]*Condensed Matter Physics Center (IFIMAC) and Departamento de Física Teórica de la Materia Condensada,*
Universidad Autónoma de Madrid, E-28049 Madrid, Spain

In the spirit of multiscale modeling, we develop a theoretical framework for spin-lattice coupling that connects, on the one hand, to *ab initio* calculations of spin-lattice coupling parameters and, on the other hand, to the magnetoelastic continuum theory. The derived Hamiltonian describes a closed system of spin and lattice degrees of freedom and explicitly conserves the total momentum, angular momentum, and energy. Using a numerical implementation that corrects earlier Suzuki-Trotter decompositions we perform simulations on the basis of the resulting equations of motion to investigate the combined magnetic and mechanical motion of a ferromagnetic nanoparticle, thereby validating our developed method. In addition to the ferromagnetic resonance mode of the spin system, we find another low-frequency mechanical response and a rotation of the particle according to the Einstein–de Haas effect. The framework developed herein will enable the use of multiscale modeling for investigating and understanding a broad range of magnetomechanical phenomena from slow to ultrafast timescales.

The spin-orbit interaction is a relativistic effect at the heart of modern spintronics [1]. It couples the electron's spin to its orbital motion and plays a central role in quantum materials, bearing high potential for future nanoelectronic devices. Its manifestations include phenomena such as magnetocrystalline anisotropy and the Dzyaloshinskii-Moriya interaction (DMI) [2,3]. While the focus in spintronics has long been on electrons or magnons as carriers of angular momentum, newer lines of research include even circularly polarized phonons to fully understand and control the flow of angular momentum in a material [4–7]. Recently, it was demonstrated that even on ultrashort timescales angular momentum can be transferred from the spin system to the lattice [8]. In the lattice, the spin angular momentum is absorbed by phonons carrying angular momentum until, on larger timescales, the macroscopic Einstein–de Haas (EdH) effect sets in [9]. A coupling between spin and lattice degrees of freedom that, beside the exchange of energy, includes the exchange of angular momentum must be based on spin-orbit coupling, the effect of which has to be taken into account for a complete description of spin-lattice dynamics (SLD).

Descriptions of spintronic phenomena are often based on spin models, which treat the lattice degrees of freedom as a heat bath and define the spin Hamiltonian with its magneto-crystalline anisotropy and DMI for a rigid lattice. Consequently, the spin angular momentum is not conserved. First attempts to develop a framework for the calculation of coupled SLD, also referred to as molecular and spin dynamics

simulations, suffer from an incomplete formulation of the spin-lattice interaction [10–13]. The works by Aßmann [13] and Strungaru [12] assume a pseudodipolar coupling that conserves the total angular momentum, a prerequisite for a well-defined spin-lattice coupling (SLC). However, it suffers from the fact that it is not linked to first-principles calculations of SLC terms, which always rest on an expansion of the spin Hamiltonian with respect to small distortions of the lattice. The works by Hellsvik *et al.* [14], Sadhukan *et al.* [15], and Mankovsky *et al.* [16] use exactly these SLC terms, that can be derived from first principles. However, these terms do not conserve the total angular momentum since they are not rotationally invariant. This inconsistency and the need for rotational invariance has already been pointed out 50 years ago in the context of the magnetoelastic (ME) theory [17,18], a continuum theory that approximates a microscopic spin-lattice model Hamiltonian on larger length scales.

In this Letter, we develop a rotationally invariant description of a spin-lattice interaction for multiscale modeling relaxing the assumption of a rigid lattice with fixed orientation. The resulting Hamiltonian is translationally and rotationally invariant, keeping total energy, momentum, and angular momentum constant. All terms can be linked to the recently developed *ab initio* methods that allow for a first-principles calculation of model parameters [14–16], opening perspectives for multiscale modeling of SLD. We also demonstrate that our spin-lattice Hamiltonian represents the discrete formulation of magnetoelastic theory and we link the microscopic parameters with the magnetoelastic constants. We show that even terms that, in a spin model, do not include any lattice distortions must transfer angular momentum to the

*markus.weissenhofer@uni-konstanz.de
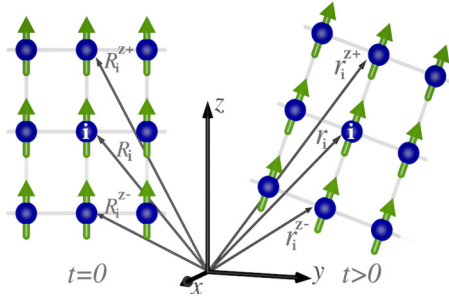
FIG. 1. Rotation and translation of a magnetized sample. The reference configuration at $t = 0$ is denoted by $\boldsymbol{R}_i$ (left), and for $t > 0$ by $\boldsymbol{r}_i$ (right). During its motion, the easy axis for an atom i at position $\boldsymbol{r}_i$ or $\boldsymbol{R}_i$ can be defined via its upper and lower neighbors at position $\boldsymbol{r}_i^{z\pm}$.

lattice. Furthermore, we derive the equations of motion for spin and lattice degrees of freedom and solve them numerically with an appropriate Suzuki-Trotter decomposition. Finally, we present simulations of the precession of a magnetized body and spin dynamics including the resulting response of the lattice.

A complete Hamiltonian accounting simultaneously for the spin and lattice degrees of freedom contains contributions from the lattice degrees of freedom (kinetic energy and pair potentials) as well as contributions which include the spin degrees of freedom. The latter can be expressed as an expansion of relativistic spin-spin interactions for small distortions [14,16],

$$
\mathcal{H}_{\text{SLC}} \approx \sum_{ij,\alpha\beta} \mathcal{J}_{ij}^{\alpha\beta} S_i^\alpha S_j^\beta + \sum_{ijk,\alpha\beta\mu} \mathcal{J}_{ij,k}^{\alpha\beta,\mu} S_i^\alpha S_j^\beta \left(u_k^\mu - u_i^\mu\right)
$$
$$
+ \sum_{ijkl,\alpha\beta\mu\nu} \mathcal{J}_{ij,kl}^{\alpha\beta,\mu\nu} S_i^\alpha S_j^\beta \left(u_k^\mu - u_i^\mu\right)\left(u_l^\nu - u_i^\nu\right), \quad (1)
$$

where the summation runs over the lattice (latin indices) and Cartesian coordinates (greek indices) [19]. $\boldsymbol{S}_i$ are unit vectors representing the direction of magnetic moments at sites i, and $\boldsymbol{u}_i = \boldsymbol{r}_i - \boldsymbol{R}_i$ are displacement vectors of atoms i at position $\boldsymbol{r}_i$ (and equilibrium position $\boldsymbol{R}_i$ in a reference configuration; see Fig. 1). The spin-spin coupling (SSC) $\mathcal{J}_{ij}^{\alpha\beta}$ and SLC tensors $\mathcal{J}_{ij,k}^{\alpha\beta,\mu} = \partial \mathcal{J}_{ij}^{\alpha\beta}/\partial u_k^\mu$ are defined with respect to a chosen coordinate system. As shown by Mankovsky *et al.*, these tensors can be calculated quantitatively from first principles [16].

The relative displacements $(u_k^\mu - u_i^\mu)$ with respect to a reference atom i take into account deformations of the lattice [20]. They are the discrete lattice representation of the strain and rotation tensor elements of elasticity theory. As such, Eq. (1) represents the discrete formulation of the ME theory [21], from which we can derive an extended expression for the ME energy density,

$$
\epsilon = \sum_{\alpha\beta\mu\nu} S^\alpha S^\beta \left(B_{\alpha\beta,\mu\nu}^s \varepsilon_{\mu\nu} + B_{\alpha\beta,\mu\nu}^{as} \omega_{\mu\nu}\right)
$$
$$
+ \sum_{\alpha\beta\gamma\mu\nu} \partial_\beta S^\alpha \partial_\gamma S^\alpha \left(A_{\beta\gamma,\mu\nu}^s \varepsilon_{\mu\nu} + A_{\beta\gamma,\mu\nu}^{as} \omega_{\mu\nu}\right)
$$
$$
+ \sum_{\alpha\beta\gamma\delta\mu\nu} \varepsilon^{\alpha\beta\gamma} S^\alpha \partial_\delta S^\beta \left(D_{\gamma\delta,\mu\nu}^s \varepsilon_{\mu\nu} + D_{\gamma\delta,\mu\nu}^{as} \omega_{\mu\nu}\right), \quad (2)
$$

where $\boldsymbol{S}$ is the continuous magnetization, $\varepsilon_{\mu\nu}$ the strain tensor, $\varepsilon^{\alpha\beta\gamma}$ the Levi-Civita symbol, and $\omega_{\mu\nu}$ the rotation tensor. The important role of the latter in the ME theory has been addressed before by Melcher [17,18], and reaffirmed in recent experiments [22–24]. The terms in Eq. (2) model anisotropy, Heisenberg exchange, and DMI due to lattice distortions and the corresponding symmetric/antisymmetric ME tensors $B_{\alpha\beta,\mu\nu}^{s/as}$, $A_{\beta\gamma,\mu\nu}^{s/as}$, and $D_{\gamma\delta,\mu\nu}^{s/as}$ can be obtained from the microscopic SLC tensors. A detailed derivation can be found in the Supplemental Material [25] as well as the connection between the ME constants [21] and the microscopic SLC tensors.

Looking at Eq. (1) one finds immediately that this Hamiltonian does not conserve the total (spin and lattice) angular momentum, since it is not rotationally invariant. It is, hence, not capable of describing spins plus lattice as a closed system. To understand this, we examine an isotropic Heisenberg model with a uniaxial on-site anisotropy,

$$
\mathcal{H}_{\text{ani}} = -\sum_{ij} J_{ij} \boldsymbol{S}_i \cdot \boldsymbol{S}_j - d_z \sum_i \left(S_i^z\right)^2, \quad (3)
$$

for a system with the z axis being the easy axis of the magnetization. Here, the Heisenberg exchange interaction term is rotationally invariant and conserves the total spin angular momentum. The anisotropy term, however, is not rotationally invariant and the total spin angular momentum is, hence, not conserved. To keep the total angular momentum conserved, the spin angular momentum would have to go to the lattice but since this term does not include any lattice degrees of freedom it cannot.

The situation is shown in Fig. 1. Let us assume the atoms are at time $t = 0$ in equilibrium positions $\boldsymbol{R}_i$ in a reference configuration with the easy axis along z (defined in the laboratory frame). When the sample starts moving the atom positions at later times are $\boldsymbol{r}_i(t) = \boldsymbol{R}_i + \boldsymbol{u}_i(t)$ and the easy axis may no longer be aligned with the z axis of the laboratory frame. Consequently, the anisotropy term in Eq. (3) has to be transformed. This can be done by projecting the spin orientation using unit vectors that are defined in terms of the respective neighbor atoms.

In a cubic lattice an appropriate unit vector $\boldsymbol{e}^z$ can be defined via the upper $(+)$ and lower $(-)$ nearest neighbors of atom i at positions $\boldsymbol{r}_i^{z\pm} = \boldsymbol{R}_i^{z\pm} + \boldsymbol{u}_i^{z\pm}$, yielding

$$
\boldsymbol{e}_i^{z(\pm)} = \frac{\boldsymbol{r}_i^{z\pm} - \boldsymbol{r}_i}{\left|\boldsymbol{r}_i^{z\pm} - \boldsymbol{r}_i\right|}. \quad (4)
$$

Now we can write the anisotropy term of Eq. (3) without reference to a specific coordinate system and we obtain

$$
\mathcal{H}_{\text{ani}} = -\sum_{ij} J_{ij} \boldsymbol{S}_i \cdot \boldsymbol{S}_j - \frac{d_z}{2} \sum_i \left[\left(\boldsymbol{S}_i \cdot \frac{\boldsymbol{r}_i^{z+} - \boldsymbol{r}_i}{\left|\boldsymbol{r}_i^{z+} - \boldsymbol{r}_i\right|}\right)^2 \right.
$$
$$
\left. + \left(\boldsymbol{S}_i \cdot \frac{\boldsymbol{r}_i^{z-} - \boldsymbol{r}_i}{\left|\boldsymbol{r}_i^{z-} - \boldsymbol{r}_i\right|}\right)^2\right]. \quad (5)
$$

The resulting Hamiltonian contains only scalar products of the spins $\boldsymbol{S}_i$ and differences of position vectors $\boldsymbol{r}_i$. It is hence translationally and rotationally invariant and will keep the total momentum and angular momentum constant. Most importantly, the transformed Hamiltonian contains the lattice

degrees of freedom explicitly, even though the original one did not. Only this makes it possible to transfer angular momentum from the spins to the lattice, keeping the total angular momentum constant.

The microscopic origin of the anisotropy can be crucial in determining the exact form of the definition of the z direction. It is however sufficient to take only two neighbors into account to capture the majority of effects. Note that this local definition of an easy axis does not only work for a global rotation but also for deformations of the sample. Furthermore, both upper and lower neighbors are used to define the local easy axis for spins i, a definition that holds also at surfaces with a reduced number of neighbors. Nevertheless, it should be stressed that this definition is neither unique nor trivial, since the choice of neighbors for the definition of the unit vectors will affect the equations of motion and the atoms the angular momentum is transferred to. Also, we want to point out that while the continuum magnetoelastic theory considers ideal homogeneous crystals, our formulation in principle allows for the inclusion of additional contributions to spin-lattice coupling that would result from a locally reduced crystal symmetry due to defects and dislocations, for which the choice of neighbors would have to be adapted depending on the local atomic arrangement.

The transformation above can be extended to other contributions of the spin-lattice Hamiltonian (1). In order to do so, the local definition for the unit vector in the z direction for atom i from Eqs. (4) can be generalized to a set of three orthogonal directions α,

$$ \boldsymbol{e}_i^{\alpha(\pm)} = \frac{\boldsymbol{r}_i^{\alpha\pm} - \boldsymbol{r}_i^{\alpha}}{\left|\boldsymbol{r}_i^{\alpha\pm} - \boldsymbol{r}_i^{\alpha}\right|}. \tag{6} $$

Similar to the case of a uniaxial anisotropy, these unit vectors can be used to transform the first term of Eq. (1),

$$ \mathcal{H}_{\mathrm{SS}} = \sum_{ij} \sum_{\alpha\beta} \mathcal{J}_{ij}^{\alpha\beta} S_i^{\alpha} S_j^{\beta} = \sum_{ij} \sum_{\alpha\beta} \mathcal{J}_{ij}^{\alpha\beta} \left(\boldsymbol{S}_i \cdot \boldsymbol{e}_i^{\alpha}\right)\left(\boldsymbol{S}_j \cdot \boldsymbol{e}_j^{\beta}\right). \tag{7} $$

Again, this Hamiltonian consists of scalar products of spins and differences of position vectors and is hence rotationally invariant. Analogously, the spin-lattice Hamiltonian becomes

$$ \mathcal{H}_{\mathrm{SLC}} = \mathcal{H}_{\mathrm{SS}} + \sum_{ijk,\alpha\beta\mu} \mathcal{J}_{ij,k}^{\alpha\beta,\mu} \left(\boldsymbol{S}_i \cdot \boldsymbol{e}_i^{\alpha}\right)\left(\boldsymbol{S}_j \cdot \boldsymbol{e}_j^{\beta}\right) $$
$$ \times \left[(\boldsymbol{r}_k - \boldsymbol{r}_i) \cdot \boldsymbol{e}_k^{\mu} - R_{ki}\right] + \cdots, \tag{8} $$

where R_{ki} is the equilibrium distance between atoms k and i in the reference configuration. This Hamiltonian consists of the rotationally invariant spin-spin term ($\mathcal{H}_{\mathrm{SS}}$) and a second spin-spin-lattice term. It should be stressed here that the choice of unit vectors does not affect the relation of the atomistic spin-lattice Hamiltonian to the continuum theory and the first-principles determination of the parameters, since this was done before the transformation on the basis of Eq. (1).

Each term in the initial formulation (1) that breaks rotational symmetry now depends on the spins and the lattice positions and, hence, can transfer angular momentum between the two subsystems. Thus, the dominating terms for angular momentum transfer may vary for different materials,

TABLE I. Maximal absolute SSC J_{ij}^{SSC} and maximal modification of SSC due to SLC $\Delta J_{ij}^{\mathrm{SLC}} = J_{ij,j} \cdot u_j^x$ (in meV) in the presence of a displacement $u_j^x = 0.03 a_{\mathrm{lat}}$ in Fe and FePt for different SSC contributions. For both materials, we consider sites i and j being Fe atoms with different distances r_{ij} and list the values for the pair ij with the largest contribution to the respective parts of the SSC tensor. In Fe, the largest contribution which can transfer angular momentum is the spin-lattice DMI $|\Delta \boldsymbol{D}_{ij}| = |\boldsymbol{D}_{ij,j}^x \cdot u_j^x|$ for $r_{ij} = 1 a_{\mathrm{lat}}$, and in FePt it is the spin-spin antisymmetric diagonal part $|J_{ij}^{\mathrm{dia-a}}| = \frac{1}{2}|J_{ij}^{xx} - J_{ij}^{zz}|$ for $r_{ij} = 1.414 a_{\mathrm{lat}}$. The symmetrized off-diagonal elements are defined as $J_{ij}^{\mathrm{off-s}} = \frac{1}{2}(J_{ij}^{xy} + J_{ij}^{yx})$. For details, see the Supplemental Material [25].

Material	Contribution to SSC	$|J_{ij}^{\mathrm{iso}}|$	$|J_{ij}^{\mathrm{dia-a}}|$	$|J_{ij}^{\mathrm{off-s}}|$	$|\boldsymbol{D}_{ij}|$
Fe	J_{ij}^{SSC}	11.389	0.019	0.017	0.0
	$\Delta J_{ij}^{\mathrm{SLC}}(u_j^x)$	1.587	0.002	0.003	0.062
FePt	J_{ij}^{SSC}	9.590	0.320	0.209	0.0
	$\Delta J_{ij}^{\mathrm{SLC}}(u_j^x)$	1.960	0.023	0.024	0.089

depending on the specific values of the SSC and SLC tensors. For example, in Fe the transfer is mainly via the spin-lattice DMI [16], whereas in FePt the dominating terms are two-site anisotropy terms (see Table I).

As an application of our formulation and to test its validity, we perform combined SLD simulations using the following Hamiltonian for a simple cubic lattice,

$$ \mathcal{H} = \mathcal{H}_{\mathrm{ani}} + \sum_i \frac{\boldsymbol{p}_i^2}{2m} + V_0 \sum_{ij} \frac{(r_{ij} - R_{ij})^2}{R_{ij}}, \tag{9} $$

that extends our rotationally invariant formulation of the spin Hamiltonian of Eq. (5) by terms describing the interaction and the kinetic energy of the lattice, with m being the mass of the atoms and V_0 describing the strength of the lattice interactions in the harmonic approximation. For the sake of simplicity, we assume that these interactions are restricted to the first three shells of neighbors and that they scale inversely with the equilibrium distance.

Evaluating the dynamics of spin and lattice degrees of freedom $\{\boldsymbol{r}_i, \boldsymbol{p}_i, \boldsymbol{S}_i\}$ requires the concurrent solution of the coupled equations of motion,

$$ \dot{\boldsymbol{r}}_i = \frac{\partial \mathcal{H}}{\partial \boldsymbol{p}_i}, \quad \dot{\boldsymbol{p}}_i = -\frac{\partial \mathcal{H}}{\partial \boldsymbol{r}_i}, \quad \text{and} \quad \dot{\boldsymbol{S}}_i = \frac{\gamma}{\mu_{\mathrm{s}}} \boldsymbol{S}_i \times \frac{\partial \mathcal{H}}{\partial \boldsymbol{S}_i}, \tag{10} $$

with γ and μ_{s} being the absolute values of the gyromagnetic ratio and the magnetic spin moment, respectively. Conservation of energy, momentum, and angular momentum can be ensured by using a symplectic algorithm. Here, we use a scheme based on the Liouville formalism [26] and the Suzuki-Trotter decomposition [27] that was initially proposed in Ref. [28] and has proven reliable for the simulation of combined SLD [10,12,13,29–32]. Note that the presence of a uniaxial on-site anisotropy term, which is quadratic in the spins, requires a further decomposition of the integration scheme that has yet to be discussed in literature. Details, tests of the conservation of the total angular momentum and the energy of the system, and a comparison of the temperature dependence of the magnetization with spin dynamics (SD)
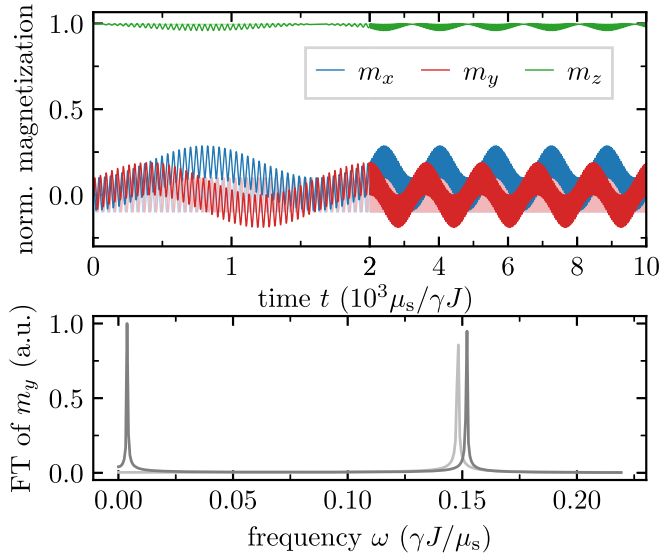
FIG. 2. Coherent magnetization dynamics of a free cubic nanoparticle obtained from SLD in comparison with SD simulations (light curves) for toy model parameters. Top: Magnetization vector components m_α vs time. Bottom: Fourier transform of m_y.

FIG. 3. Mechanical motion of a cubic nanoparticle excited by coherent precession of the magnetization around n_3 (easy axis). (a) Spiraling magnetization dynamics and easy-axis precession in the time interval $[0, 10^3]\mu_s/\gamma J$ for toy model parameters. (b) Sketch of the two characteristic mechanical modes. (c) Characteristic frequencies of an FePt nanoparticle vs cube size l. Dotted lines correspond to theory curves for ω_{FMR} and ω_{n_3} as explained in the text and a guide to the eye for ω_{EdH}.

simulations based on the stochastic Landau-Lifshitz-Gilbert equation of motion can be found in the Supplemental Material [25].

As an application we study the coupled magnetization and lattice dynamics of a free cubic nanoparticle using toy model parameters as well as realistic parameters modeling $L1_0$ FePt [25]. For this simulation we assume that initially the cube is oriented such that the easy axis is aligned with the z axis and all spins point along $\boldsymbol{m}_0 = (0.1, 0, \sqrt{1 - 0.1^2})^T$. This gives rise to a coherent precession of the magnetization along with mechanical motion of the cube. We begin by discussing the general aspects of the emerging dynamics based on toy model parameters, since for real materials, the timescales of magnetic and mechanical motion can be very different (see below). Figure 2 displays the time evolution of the magnetization $\boldsymbol{m} = \frac{1}{N} \sum_i^N \boldsymbol{S}_i$ and the Fourier transform of its y component for a nanoparticle consisting of 4^3 atoms. The light curves are obtained by pure SD simulations, for which we keep the position of the atoms fixed. In contrast to pure SD, the SLD simulations produce oscillations at two characteristic frequencies $\omega_{n_3} \approx 3.89 \times 10^{-3}\gamma J/\mu_s$ and $\omega_{FMR} \approx 0.152\gamma J/\mu_s$. The peak at ω_{FMR} can be attributed to the usual ferromagnetic resonance (FMR) frequency and is close to the value predicted by linear spin-wave theory $\omega_{FMR} = 2\bar{d}\gamma/\mu_s = 0.15\gamma J/\mu_s$, where $\bar{d}$ is the averaged uniaxial magnetic anisotropy [33]. The SD value ($\omega_{FMR} \approx 0.148\gamma J/\mu_s$) is slightly smaller due to finite-size effects: The spins at the edges of the cube lag behind, since their anisotropy field is weaker [cf. Eq. (5)], slowing down the overall precession frequency. Surprisingly, the FMR frequency of SLD is shifted to higher values as compared to the SD value.

The emergence of the peak at ω_{n_3} as well as the shift of the FMR frequency are a result of the mechanical motion of the nanoparticle, which can be characterized by the vectors $\boldsymbol{n}_\alpha$ ($\alpha \in 1, 2, 3$) normal to the faces of the cube. As the easy

axis is firmly attached to one of these vectors (without loss of generality, $\boldsymbol{n}_3$), we can compare the dynamics of the easy axis and the magnetization [see Fig. 3(a)]. We find that the magnetization precesses around the easy axis, which itself revolves around $\boldsymbol{m}_0$ exactly at ω_{n_3}, giving rise to the second peak in Fig. 2 and the shift of the FMR frequency.

This emergence of the easy-axis precession was predicted in Ref. [34] based on a simple rigid-body-macrospin model [35–37]. There, the magnetic nanoparticle is described by the normalized magnetization $\boldsymbol{m}$ and the vectors $\boldsymbol{n}_\alpha$ introduced above. The dynamics of these vectors $\boldsymbol{n}_\alpha$ are given by $\dot{\boldsymbol{n}}_\alpha = \boldsymbol{\omega} \times \boldsymbol{n}_\alpha$, where $\boldsymbol{\omega}$ is the angular velocity of the nanoparticle in the laboratory frame, which is related to its angular momentum via $\boldsymbol{L} = \Theta\boldsymbol{\omega}$. For a cubic nanoparticle, the moment of inertia is given by $\Theta = \frac{1}{6}Nml^2$, l being the cube size and N being the number of atoms. Conservation of angular momentum requires that $-N\frac{\mu_s}{\gamma}\dot{\boldsymbol{m}} + \dot{\boldsymbol{L}} = 0$. If the nanoparticle is initially at rest, we get $\boldsymbol{\omega}(t) = \frac{6\mu_s}{ml^2\gamma}[\boldsymbol{m}(t) - \boldsymbol{m}_0]$, with $\boldsymbol{m}_0$ being the initial orientation of the magnetization. This yields $\dot{\boldsymbol{n}}_\alpha = \frac{6\mu_s}{ml^2\gamma}[\boldsymbol{m}(t) \times \boldsymbol{n}_\alpha - \boldsymbol{m}_0 \times \boldsymbol{n}_\alpha]$. The first contribution to the torque depends on the current value of the magnetization and amounts to zero for $\boldsymbol{n}_3$, due to the rapid oscillations of $\boldsymbol{m}(t)$ around $\boldsymbol{n}_3$. The second term describes a simple rotation of $\boldsymbol{n}_3$ around the initial direction of the magnetization $\boldsymbol{m}_0$ with frequency $\omega_{n_3} = \frac{6\mu_s}{ml^2\gamma}$. For the parameters used here, we calculate $\omega_{n_3} \approx 3.75 \times 10^{-3}\gamma J/\mu_s$, which is in close agreement with the simulation results.

In addition to the precession of $\boldsymbol{n}_3$, we find an EdH-type rotation of $\boldsymbol{n}_{1,2}$ with $\omega^{EdH} \approx 1.81 \times 10^{-5}\gamma J/\mu_s$ around the z axis of the laboratory frame [see Fig. 3(b)]. This rotation

occurs when the average magnetization differs from its initial value, since the average angular velocity of the cubic nanoparticle is given by $\langle\boldsymbol{\omega}(t)\rangle = \frac{6\mu_s}{ml^2\gamma}\langle(\boldsymbol{m}(t) - \boldsymbol{m}_0)\rangle$. This leads to a nonzero value only for the z component of the angular velocity (cf. Fig. 2).

Figure 3(c) displays all three characteristic frequencies versus cube size for parameters modeling $L1_0$ FePt nanoparticles. Again, the FMR frequency is the highest and approaches the bulk value for large cubes. The other two (mechanical) frequencies are more than three orders of magnitude lower and scale with l^{-2}, while keeping a constant ratio of around 0.004 over the range considered here [38]. Besides testing the validity of the analytical expression for ω_{n_3}, this allows us to estimate the mechanical frequencies for larger particles. For example, for an FePt nanocube with edge length of 100 nm we get $\omega_{n_3} \approx 250\,\text{kHz}$ and $\omega_{\text{EdH}} \approx 1\,\text{kHz}$.

In summary, we have developed a rotationally invariant formulation of coupled spin-lattice dynamics for multiscale modeling of magnetomechanical motion. It successfully integrates first-principles evaluation of SLC parameters, ME continuum theory, and spin-lattice dynamics simulations.

Employing our developed framework and a numerical implementation that corrects earlier Suzuki-Trotter decompositions we simulate combined magnetomechanical dynamics of a ferromagnetic nanoparticle, thereby validating our formulation. Our simulations demonstrate that in addition to the ferromagnetic resonance mode of the spin system there are two low-frequency mechanical modes describing the precession of the easy axis and a rotation of the particle according to the EdH effect. By incorporating total angular momentum conservation, our work provides the tools for simulation of a broad range of magnetomechanical phenomena. Therefore it is crucial to the understanding of recent and ongoing intriguing experiments, e.g., on magnon-phonon coupling or ultrafast magnetization dynamics.

[1] A. Manchon, H. C. Koo, J. Nitta, S. M. Frolov, and R. A. Duine, Nat. Mater. **14**, 871 (2015).

[2] I. Dzyaloshinsky, J. Phys. Chem. Solids **4**, 241 (1958).

[3] T. Moriya, Phys. Rev. **120**, 91 (1960).

[4] A. Hirohata, K. Yamada, Y. Nakatani, I.-L. Prejbeanu, B. Diény, P. Pirro, and B. Hillebrands, J. Magn. Magn. Mater. **509**, 166711 (2020).

[5] D. A. Garanin and E. M. Chudnovsky, Phys. Rev. B **92**, 024421 (2015).

[6] A. Rückriegel, S. Streib, G. E. W. Bauer, and R. A. Duine, Phys. Rev. B **101**, 104402 (2020).

[7] J. H. Mentink, M. I. Katsnelson, and M. Lemeshko, Phys. Rev. B **99**, 064428 (2019).

[8] S. R. Tauchert, M. Volkov, D. Ehberger, D. Kazenwadel, M. Evers, H. Lange, A. Donges, A. Book, W. Kreuzpaintner, U. Nowak, and P. Baum, Nature (London) **602**, 73 (2022).

[9] C. Dornes, Y. Acremann, M. Savoini, M. Kubli, M. J. Neugebauer, E. Abreu, L. Huber, G. Lantz, C. A. F. Vaz, H. Lemke, E. M. Bothschafter, M. Porer, V. Esposito, L. Rettig, M. Buzzi, A. Alberca, Y. W. Windsor, P. Beaud, U. Staub, D. Zhu *et al.*, Nature (London) **565**, 209 (2019).

[10] P.-W. Ma and C. H. Woo, Phys. Rev. E **79**, 046703 (2009).

[11] D. Perera, M. Eisenbach, D. M. Nicholson, G. M. Stocks, and D. P. Landau, Phys. Rev. B **93**, 060402(R) (2016).

[12] M. Strungaru, M. O. A. Ellis, S. Ruta, O. Chubykalo-Fesenko, R. F. L. Evans, and R. W. Chantrell, Phys. Rev. B **103**, 024429 (2021).

[13] M. Aßmann and U. Nowak, J. Magn. Magn. Mater. **469**, 217 (2019).

[14] J. Hellsvik, D. Thonig, K. Modin, D. Iuşan, A. Bergman, O. Eriksson, L. Bergqvist, and A. Delin, Phys. Rev. B **99**, 104302 (2019).

[15] B. Sadhukhan, A. Bergman, Y. O. Kvashnin, J. Hellsvik, and A. Delin, Phys. Rev. B **105**, 104418 (2022).

[16] S. Mankovsky, S. Polesya, H. Lange, M. Weißenhofer, U. Nowak, and H. Ebert, Phys. Rev. Lett. **129**, 067202 (2022).

[17] R. L. Melcher, Phys. Rev. Lett. **25**, 1201 (1970).

[18] R. L. Melcher, Phys. Rev. Lett. **28**, 165 (1972).

[19] In this notation Eq. (1) also includes on-site terms (where $i = j$).

[20] Note that in the work of Mankovsky *et al.* [16] these tensors are calculated taking only one displacement at site k into account while all the other atoms are in their equilibrium position. In this case the relative displacement is $u_k^\mu - u_i^\mu = u_k^\mu$. However, for a system that is displaced as a whole (equally for all sites i) the relative displacement will vanish and there is no additional contribution to the potential energy.

[21] C. Kittel, Rev. Mod. Phys. **21**, 541 (1949).

[22] M. Xu, K. Yamamoto, J. Puebla, K. Baumgaertl, B. Rana, K. Miura, H. Takahashi, D. Grundler, S. Maekawa, and Y. Otani, Sci. Adv. **6**, eabb1724 (2020).

[23] M. Küß, M. Heigl, L. Flacke, A. Hörner, M. Weiler, M. Albrecht, and A. Wixforth, Phys. Rev. Lett. **125**, 217203 (2020).

[24] M. Küß, M. Albrecht, and M. Weiler, Front. Phys. **10**, 981257 (2022).

[25] See Supplemental Material at http://link.aps.org/supplemental/10.1103/PhysRevB.108.L060404 for (i) a detailed derivation of the continuum magnetoelastic theory relating its parameters to those obtained from first-principles calculations, (ii) details on the numerical simulation, and (iii) evaluation of the magnetoelastic tensors using first-principles calculation, which includes Refs. [39–57].

[26] D. Frenkel and B. Smit, *Understanding Molecular Simulation: From Algorithms to Applications* (Elsevier, Amsterdam, 2001), Vol. 1.

[27] M. Suzuki, Commun. Math. Phys. **51**, 183 (1976).

[28] I. P. Omelyan, I. M. Mryglod, and R. Folk, Phys. Rev. Lett. **86**, 898 (2001).

[29] S.-H. Tsai, H. K. Lee, and D. P. Landau, Am. J. Phys. **73**, 615 (2005).

[30] P.-W. Ma, S. Dudarev, and C. Woo, Comput. Phys. Commun. **207**, 350 (2016).

[31] W. Dednam, C. Sabater, A. Botha, E. Lombardi, J. Fernández-Rossier, and M. Caturla, Comput. Mater. Sci. **209**, 111359 (2022).

[32] J. R. Cooke and J. R. Lukes, Phys. Rev. B **107**, 024419 (2023).

[33] Given the form of the anisotropy in Eq. (5), the effective uniaxial anisotropy of spins at two faces of the cube is reduced by a factor of two. Thus, for a cube consisting of 4^3 atoms, we calculate $\bar{d} = 0.75d_z$.

[34] N. Usov and B. Y. Liubimov, J. Magn. Magn. Mater. **385**, 339 (2015).

[35] N. A. Usov and B. Y. Liubimov, J. Appl. Phys. **112**, 023901 (2012).

[36] K. D. Usadel and C. Usadel, J. Appl. Phys. **118**, 234303 (2015).

[37] H. Keshtgar, S. Streib, A. Kamra, Y. M. Blanter, and G. E. W. Bauer, Phys. Rev. B **95**, 134447 (2017).

[38] Note that for cube sizes larger than $12a$, ω_{EdH} leads to a rotation of less than $3°$ on the timescale of the simulation. This makes its extraction from simulation data difficult and probably is the cause of its fluctuations for larger cube sizes.

[39] R. LeCraw and R. Comstock, in *Lattice Dynamics*, edited by W. P. Mason, Physical Acoustics Vol. 3 (Academic, New York, 1965), pp. 127–199.

[40] A. G. Gurevich and G. A. Melkov, *Magnetization Oscillations and Waves* (CRC Press, Boca Raton, FL, 2020).

[41] L. Exl, D. Suess, and T. Schrefl, in *Handbook of Magnetism and Magnetic Materials*, edited by M. Coey and S. Parkin (Springer, Cham, 2020), pp. 1–44.

[42] D. Lewis and N. Nigam, J. Comput. Appl. Math. **151**, 141 (2003).

[43] O. N. Mryasov, U. Nowak, K. Y. Guslienko, and R. W. Chantrell, Europhys. Lett. **69**, 805 (2005).

[44] J. B. Staunton, L. Szunyogh, A. Buruzs, B. L. Gyorffy, S. Ostanin, and L. Udvardi, Phys. Rev. B **74**, 144411 (2006).

[45] S. Couet, M. Sternik, B. Laenens, A. Siegel, K. Parlinski, N. Planckaert, F. Gröstlinger, A. I. Chumakov, R. Rüffer, B. Sepiol, K. Temst, and A. Vantomme, Phys. Rev. B **82**, 094109 (2010).

[46] J. Barker, R. F. L. Evans, R. W. Chantrell, D. Hinzke, and U. Nowak, Appl. Phys. Lett. **97**, 192504 (2010).

[47] A. Einstein and W. J. de Haas, Verhandl. Deut. Phys. Ges. **17**, 152 (1915).

[48] M. O. A. Ellis and R. W. Chantrell, Appl. Phys. Lett. **106**, 162407 (2015).

[49] L. Rózsa, S. Selzer, T. Birk, U. Atxitia, and U. Nowak, Phys. Rev. B **100**, 064422 (2019).

[50] H. Ebert, The Munich SPR-KKR package, version 8.5, https://www.ebert.cup.uni-muenchen.de/en/software-en/13-sprkkr (2020).

[51] H. Ebert, D. Ködderitzsch, and J. Minár, Rep. Prog. Phys. **74**, 096501 (2011).

[52] A. I. Liechtenstein, M. Katsnelson, V. Antropov, and V. Gubanov, J. Magn. Magn. Mater. **67**, 65 (1987).

[53] H. Ebert and S. Mankovsky, Phys. Rev. B **79**, 045209 (2009).

[54] L. Udvardi, L. Szunyogh, K. Palotás, and P. Weinberger, Phys. Rev. B **68**, 104436 (2003).

[55] M. E. Rose, *Relativistic Electron Theory* (Wiley, New York, 1961).

[56] N. Papanikolaou, R. Zeller, P. H. Dederichs, and N. Stefanou, Phys. Rev. B **55**, 4157 (1997).

[57] S. H. Vosko, L. Wilk, and M. Nusair, Can. J. Phys. **58**, 80 (1980).